Catalysis Today xxx (2013) xxx–xxx

Contents lists available at SciVerse ScienceDirect

Catalysis Today

journal homepage: www.elsevier.com/locate/cattod

Stability and regeneration of Cu–ZrO_2 catalysts used in glycerol hydrogenolysis to 1,2-propanediol

D. Durán-Martín, M. Ojeda, M. López Granados, J.L.G. Fierro, R. Mariscal*

Group of Sustainable Energy and Chemistry (EQS), Institute of Catalysis and Petrochemistry (ICP-CSIC), C/Marie Curie 2, Cantoblanco, 28049 Madrid, Spain

ARTICLE INFO

Article history:
Received 29 September 2012
Received in revised form
27 November 2012
Accepted 28 November 2012
Available online xxx

Keywords:
Glycerol
Hydrogenolysis
CuZr catalysts
Coprecipitation
Regeneration

ABSTRACT

A series of Cu–ZrO_2 catalysts with different copper contents have been prepared by the coprecipitation method. Their catalytic behavior was studied for glycerol hydrogenolysis reaction to obtain 1,2-propanediol (1,2-PDO) joint to deactivation mechanism and regeneration protocols. A number of physical chemical techniques as X-ray diffraction (XRD), evolved gas analysis by mass spectrometry (EGA-MS), temperature programmed reduction (TPR), X-ray photoelectron spectroscopy (XPS) and chemical analysis have been used to characterize the precursors, activated and spent catalysts. Cu–ZrO_2 catalysts with higher atomic ratio Cu/Zr showed higher selectivity while glycerol conversion values were not significantly changed. In terms of stability a decreasing of yield to 1,2-PDO due to a decrease of its selectivity was observed with the number of cycles. The main cause of deactivation was associated to the progressive formation of organic deposits on the surface of catalyst. A regeneration process highly efficient, where almost complete recovery of yield to 1,2-PDO shown by the fresh catalyst was reached, has been identified.

© 2012 Elsevier B.V. All rights reserved.

1. Introduction

Glycerol is obtained in very large quantities as an inevitable co-product during fatty acid methyl esters (FAME, biodiesel) synthesis *via* triglycerides transesterification with methanol. This has caused glycerol to be currently an available and inexpensive building block with high potential to prepare a large variety of other chemicals with high added value. A relevant and attractive glycerol valorization route from industry and academic points of view consists in its chemical transformation into propanediols *via* hydrogenolysis reactions with solid catalysts [1,2].

In this context, Cu-based catalysts, either as bulk [3–5] or supported [6–9] materials, have shown excellent catalytic properties for the specific glycerol hydrogenolysis to 1,2-propanediol (1,2-PDO). More specifically, coprecipitated Cu–ZnO binary systems have been previously reported as efficient catalysts for 1,2-PDO synthesis from glycerol/H_2O mixtures at 453–513 K and 2–8 MPa H_2 [3,4]. However, our recent investigations show that these catalytic systems deactivate under typical reaction conditions (473 K, 4 MPa H_2) because of significant leaching phenomena of Zn species into the liquid phase (pH <7) and subsequent Cu sintering [10].

To improve the stability of these Cu-based materials during liquid phase glycerol hydrogenolysis to 1,2-PDO, we have explored the use of ZrO_2 instead of ZnO in Cu-based catalysts as a route to avoid Cu agglomeration during the catalytic reaction. As for ZnO, ZrO_2 exhibits an excellent thermal stability, identical structural features (hexagonal phase), comparable ionic radii (0.80 and 0.74 Å for Zr^{4+} and Zn^{2+}, respectively), and similar acid–base properties. In contrast, ZrO_2 shows an increased resistance to acid attack (higher chemical inertness), which would ultimately prevent Cu sintering. All these features led us to explore the use of CuZr systems as promising catalysts for glycerol hydrogenolysis reactions in liquid phase.

Here, we report our investigations on the use of coprecipitated CuZr oxides as catalysts for glycerol hydrogenolysis to 1,2-PDO in liquid phase. To the best of our knowledge, these materials have not been previously employed as catalysts in glycerol hydrogenolysis at industrial relevant conditions (liquid phase and H_2 pressures below 5.0 Mpa). More precisely, we have determined the chemical composition (Cu/Zr molar ratio) that leads to the highest yields to 1,2-PDO at milder reaction conditions. We have also identified the different deactivation mechanisms that occur during glycerol hydrogenolysis, and have found an appropriate catalyst regeneration protocol that allows a substantial recovery of the initial high selectivity.

2. Experimental

2.1. Catalysts preparation and activation protocols

A series of CuZr solids with different Cu/Zr atomic ratios was prepared by co-precipitation. $Cu(NO_3)_2{\cdot}2H_2O$ (Fluka, >98%) and

* Corresponding author. Tel.: +34 91 5854938; fax: +34 91 5854760.
E-mail address: r.mariscal@icp.csic.es (R. Mariscal).

0920-5861/$ – see front matter © 2012 Elsevier B.V. All rights reserved.
http://dx.doi.org/10.1016/j.cattod.2012.11.013

Please cite this article in press as: D. Durán-Martín, et al., Stability and regeneration of Cu–ZrO_2 catalysts used in glycerol hydrogenolysis to 1,2-propanediol, Catal. Today (2013), http://dx.doi.org/10.1016/j.cattod.2012.11.013

$ZrO(NO_3)_2{\cdot}xH_2O$ (Sigma–Aldrich, 99.9% metal) were dissolved in deionized water (0.3 M total metal content) to achieve nominal Cu/Zr atomic ratios of 0.2, 0.4, 1, 2.5, and 6. The mixture was stirred at room temperature and constant pH = 7 by adding an aqueous Na_2CO_3 solution (0.5 M). Once the precipitation was over, the precipitate was aged in the mother liquor under these conditions for 4 h, and the solid was subsequently recovered by filtration and washed with deionized H_2O. The catalytic precursors are named here as *x*CuZr-*p*, where *x* denotes the Cu/Zr atomic ratio. Monometallic samples (denoted as Cu-*p* and ZrO_2-*p*) were also prepared following identical protocols.

The precursors were first treated in flowing synthetic air at 673 K (heating rate of 10 K min^{-1}) for 1 h and then in H_2/Ar (5 vol.% H_2) at 573 K (heating rate of 5 K min^{-1}) for 1 h. The conditions of the treatment protocols were selected based on characterization results (shown later). The obtained bimetallic solids are denoted as *x*CuZr, while monometallic samples are named as Cu and ZrO_2.

2.2. Glycerol hydrogenolysis measurements

Glycerol hydrogenolysis was performed in a stainless steel Parr reactor (100 cm^3). First, the activated catalyst (~0.6 g) and an aqueous glycerol solution (25 g, 40 wt.% glycerol) were loaded into the reactor, and the system was then purged three times consecutively with N_2 and H_2. Subsequently, the temperature was increased to 473 K and H_2 pressure adjusted to 4.0 MPa. Finally, the mixture was stirred at 500 rpm to start the reaction, which was conducted for a period of 8 h. Reaction products were analyzed with a gas chromatograph (GC) equipped with a capillary column (ZB-WAX, 30 m × 320 μm × 0.5 μm) connected to a flame ionization detector. Before GC analysis, samples were prepared by adding acetone (10 g, solvent) and ethyl valerate (0.2 g, internal standard) to the reaction aliquot (0.4 g). Glycerol conversion is defined as the ratio between moles of glycerol consumed in the reaction to the total moles of glycerol initially present. Yield to 1,2-PDO is defined as the ratio of moles of product formed to the total moles of glycerol initially present, being the selectivity defined as the result of dividing the yield value by glycerol conversion calculated previously. H_2O content in the reaction products was determined by Karl Fisher titration of an aliquot of reaction highly diluted with pure methanol.

2.3. Characterization techniques

Powder X-ray diffraction (XRD) patterns were recorded in the 10–80° 2θ range in scan mode (0.02°, 1 s) using a X'Pert Pro PANalytical diffractometer with Cu Kα_1 (λ = 0.154046 nm) radiations. The crystallite size (D) was calculated by Scherrer equation, $D = 0.90\,\lambda/\beta\cos\theta$, where θ is the diffraction angle and β is the full width at half-maximum (FWHM).

Evolved gas analysis by mass spectrometry (EGA-MS) was performed by loading the samples (*ca.* 0.1 g) in a U-shaped quartz reactor connected to a Balzer Prisma™ quadrupole mass spectrometer (QMS 200). The analysis was conducted while flowing an O_2/Ar mixture (50 cm^3 min^{-1}, 20 vol.% O_2) from room temperature to 1000 K at a heating rate of 10 K min^{-1}. The fragments m/z = 18 (H_2O^+) and 44 ($CO_2{}^+$) were continuously monitored with the mass spectrometer. Gas lines from the reactor outlet to the MS inlet were heated to 393 K to avoid H_2O condensation phenomena. Temperature-programmed reduction (TPR) experiments were also performed with the U-shaped reactor connected to the mass spectrometer. A H_2/Ar mixture (5 vol. % H_2/Ar) was contacted with the sample while heating from room temperature to 1000 K at a rate of 5 K min^{-1}.

X-ray photoelectron spectroscopy (XPS) spectrum were recorded with a VG Escalab 200 R Fisons spectrometer equipped with Al-Kα (hν = 1486.6 eV) and Mg-Kα (hν = 1253.6 eV) X-ray sources. Binding energies were calibrated relative to the C 1s peak from adventitious carbon of the samples at 284.6 eV to correct the potential contact differences between the sample and the sample holder of spectrometer. Both binding energy (BE) values and peak areas were computed by fitting the experimental spectra to Gaussian/Lorentzian lines after removing the S-shaped background. Surface atomic ratios were calculated from the peak area ratios normalized by atomic sensitivity factors.

Chemical analysis of liquid product after reaction was carried out in Elan 6000 Perkin-Elmer Sciex inductively coupled plasma mass spectrometry. Samples were digested in open glass by a mixture of HNO_3 and H_2O_2. Afterwards, samples were diluted in 1 v/v% HNO_3. Total reflection X-ray fluorescence (TXRF) analysis was employed to determine the composition of the solids before and after reaction. Previously, samples were ground (particle size <30 mm) and homogenized with high-purity water by ultrasonic disaggregation to disperse the possible agglomeration of particles. Two microliters of the suspension was placed on a flat carrier where the water was evaporated off under a vacuum.

Table 1
Chemical analysis of CuZr precursors and CuO and Cu crystallites sizes for calcined and reduced samples respectively calculated by applying the Scherrer equation.

Sample	Cu/Zr atomic ratio by TXRF	Crystallite size (nm)	
		CuO	Cu
ZrO_2	–	n.d.	n.d.
0.2CuZr	0.2	n.d.	n.d.
0.4CuZr	0.5	n.d.	4.5
1CuZr	1.1	7.1	23.8
2.5CuZr	2.6	8.0	25.8
6CuZr	5.0	9.4	29.8
Cu	–	11.7	48.9

n.d.: not determined.

3. Results and discussion

3.1. Characterization of catalytic precursors

Table 1 shows in the first column the Cu/Zr atomic ratios for the different precursors as measured by TXRF. In general, the experimental Cu/Zr atomic ratio is in all cases quite close to nominal ones (within a 15% deviation) that indicate that precipitation of both Cu and Zn nitrates has been quantitative.

Fig. 1 shows the XRD patterns recorded with the coprecipitated CuZr samples. The Cu-free and low Cu content solids (ZrO_2-*p*, 0.2CuZr-*p*, and 0.4CuZr-*p*) exhibit a broad diffraction peak (2θ = 20–40°) attributed to low-crystalline zirconium hydroxycarbonate (1, $Zr(CO_3)(OH)_2$) [11,12], however its intensity is very small, see multiplicity factor for these diffractograms. As the Cu concentration increases (1CuZr-*p*, 2.5CuZr-*p*, 6CuZr-*p*, and Cu-*p*), diffraction lines assigned to $Cu_2(CO_3)(OH)_2$ (2, malachite; JCPDS 010-0399) are clearly observed, although the presence of $CuCO_3$ (3, JCPDS 046-0858) cannot be discarded because these two phases show similar XRD patterns. Additionally, $Cu_2(NO_3)(OH)_3$ (4, gerhardtite; JCPDS 15-0014) is also detected in the Cu-*p* sample.

The thermal decomposition of these catalytic precursors (Cu and Zr carbonates and hydroxycarbonates) in synthetic air has been explored by evolved gas analysis with mass spectrometry (EGA-MS) with the aim of determining the temperature required to form the corresponding oxides. Fig. 2 depicts the evolution of fragments with m/z = 18 and 44 (associated to H_2O and CO_2 formation, respectively). The Cu-free and low Cu content solids (ZrO_2-*p*, 0.2CuZr-*p*, and 0.4CuZr-*p*) exhibit a broad H_2O evolution process (350–475 K) with two maxima that are shifted to lower temperatures as the Cu content increases (Fig. 2a). Minor CO_2 formation (Fig. 2b) is

Please cite this article in press as: D. Durán-Martín, et al., Stability and regeneration of Cu–ZrO_2 catalysts used in glycerol hydrogenolysis to 1,2-propanediol, Catal. Today (2013), http://dx.doi.org/10.1016/j.cattod.2012.11.013

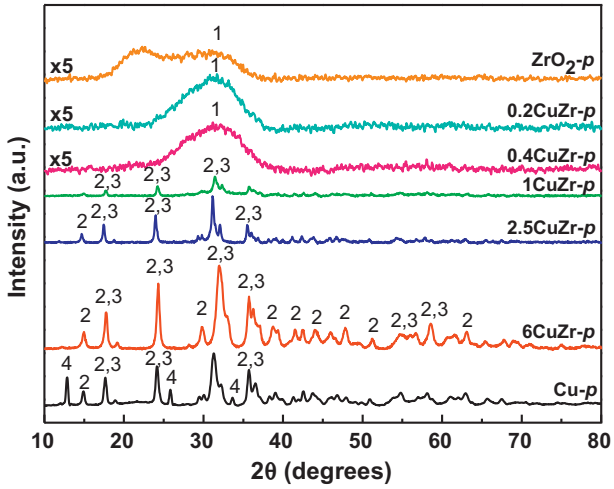

Fig. 1. XRD patterns of the co-precipitated CuZr precursors. Phases identification: (1) low-crystalline Zr hydroxycarbonate; (2) $Cu_2(CO_3)(OH)_2$; (3) $CuCO_3$; (4) $Cu_2(NO_3)(OH)_3$.

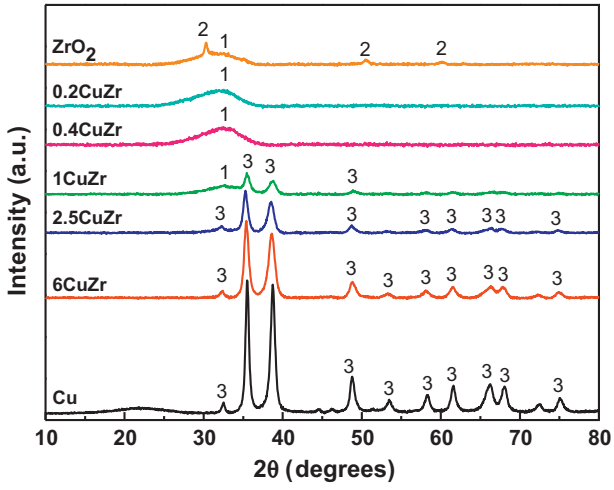

Fig. 3. XRD patterns of the *x*CuZr solids treated in synthetic air at 673 K for 1 h. Phases identification: (1) low-crystalline ZrO_2; (2) cubic ZrO_2; (3) CuO.

also detected at similar temperatures. Solids with higher Cu content (1CuZr-*p*, 2.5CuZr-*p*, 6CuZr-*p*, and Cu-*p*) depict an intense H_2O emission peak centered at 620–635 K (Fig. 2a), associated also to CO_2 formation at *ca.* 605 K (Fig. 2b), which results from hydroxycarbonates decomposition. Additionally, Cu-*p* shows also a relatively small CO_2 formation peak at 510 K. A decomposition process that released exclusively CO_2 is observed at much higher temperatures (900–930 K), a phenomenon that is related to the decomposition of carbonate precursors. In summary, EGA-MS results indicate that temperatures as high as 900 K are required to fully decompose the precursors (Cu and Zr hydroxycarbonates and carbonates). However, these severe treatments may induce the agglomeration of the resulting copper oxide particles, which would exhibit negative impact on measured catalytic activities. Therefore, all the catalytic precursors were treated in synthetic air at 673 K for 1 h, this temperature is marked by one line in Fig. 2, which ensures an extensive decomposition of Cu and Zr hydroxycarbonates (most abundant phases formed during coprecipitation).

Fig. 3 shows the XRD patterns recorded with the air-treated CuZr samples. The Cu-free and low Cu content solids (ZrO_2, 0.2CuZr, and 0.4CuZr) exhibit a broad diffraction peak ($2\theta = 20–40^\circ$) attributed to amorphous ZrO_2, although minor concentrations of crystalline cubic ZrO_2 (2, JCPDS 027-0997) is also detected in the Cu-free sample. As the Cu concentration increases (1CuZr, 2.5CuZr, 6CuZr, and Cu), only diffraction lines unequivocally assigned to crystalline CuO (3, JCPDS 041-0254) become more evident. The absence of XRD peaks attributed to carbonates species, which required temperatures higher than 900 K to decompose, reveals that these species are amorphous and consequently, undetectable by XRD. CuO crystallites sizes (1CuZr, 2.5CuZr, 6CuZr, and Cu samples) were calculated by applying the Scherrer equation to the diffraction line at $2\theta = 35.5^\circ$ (Table 1). It was found that the size of CuO particles slightly increases with the Cu/Zr atomic ratio.

The reducibility properties of the air-treated samples (*x*CuZr) and the temperature required to form metallic Cu^0 species were determined by temperature programmed reduction (TPR) in H_2/Ar (5 vol.% H_2) followed by mass spectrometry (Fig. 4). ZrO_2 shows a small H_2 consumption peak at 525 K that reveals that zirconia is partially reduced, consistent with previous reports [13–15]. CuO particles in the monometallic sample are reduced at *ca.* 500 K. Bimetallic *x*CuZr samples present in most cases two

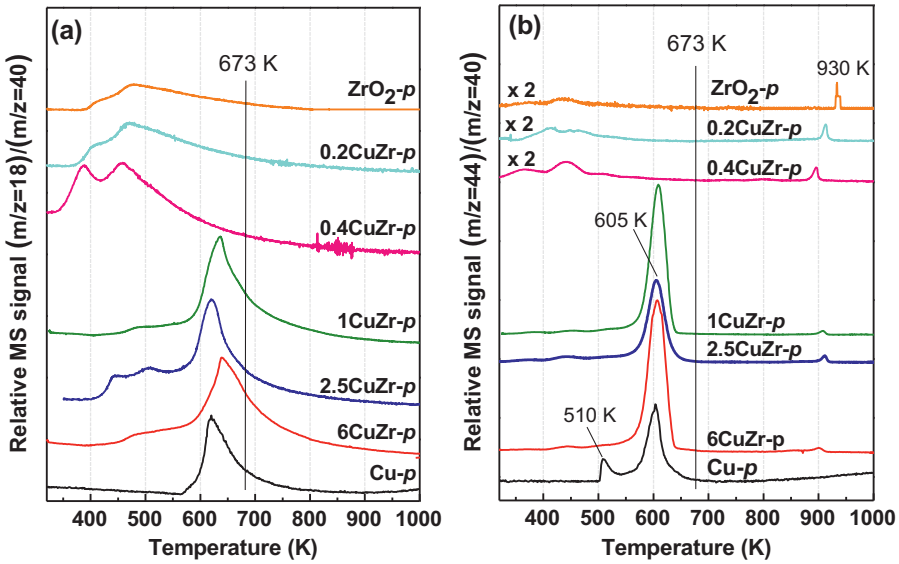

Fig. 2. EGA-MS profiles obtained during O_2/Ar treatment (20 vol.% O_2) of the coprecipitated CuZr precursors. (a) $m/z = 18$, H_2O^+; (b) $m/z = 44$, CO_2^+.

Please cite this article in press as: D. Durán-Martín, et al., Stability and regeneration of Cu–ZrO_2 catalysts used in glycerol hydrogenolysis to 1,2-propanediol, Catal. Today (2013), http://dx.doi.org/10.1016/j.cattod.2012.11.013

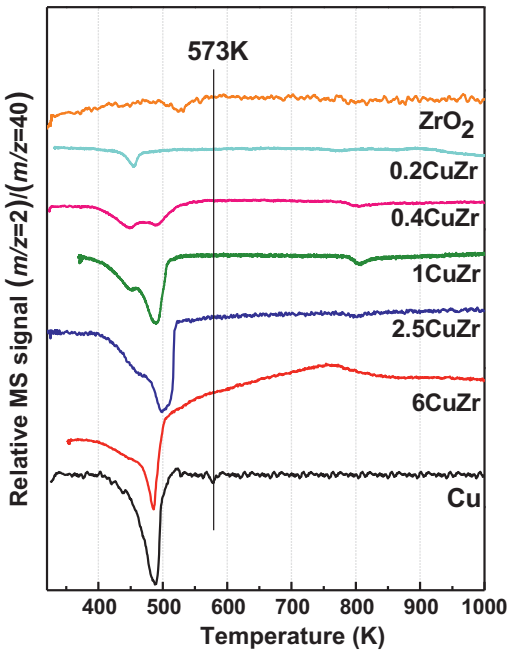

Fig. 4. H_2-TPR profiles obtained with the *x*CuZr solids (5 vol. % H_2/Ar, 5 K min^{-1}).

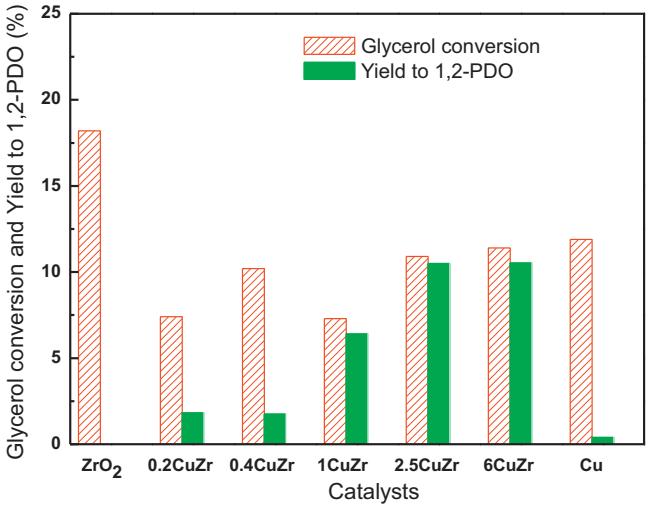

Fig. 5. Catalytic performance shown by the *x*CuZr solids in glycerol hydrogenolysis reactions (10 g glycerol, 15 g H_2O, 4.0 MPa H_2, 0.6 g catalyst, 473 K, 8 h).

reduction processes at 450 and 490 K. Based on these results, all the samples were treated in H_2/Ar at 573 K for 1 h in order to form the catalytically active species and ensure the reduction of copper oxides. Some authors have reported that the double H_2 consumption process results from the reduction of CuO to metallic Cu in two consecutive steps ($CuO \rightarrow ½\ Cu_2O \rightarrow Cu$) [16–18]. In contrast, other authors have proposed that the two H_2 consumption processes reveal the presence of different CuO species [19], with large crystalline CuO particles requiring higher temperatures than small amorphous CuO particles to be reduced. As shown in Fig. 4, the high-temperature H_2 consumption process increases with the Cu/Zr atomic ratio at expenses of low-temperature peak, consistent with the XRD patterns shown in Fig. 3 that revealed that CuO particles size increased with Cu content.

3.2. Catalytic activity and characterization of CuZr samples in glycerol hydrogenolysis

Fig. 5 summarizes the catalytic behavior shown by the CuZr reduced samples in glycerol hydrogenolysis. ZrO_2 displayed the highest glycerol conversion values (*ca.*18%) under our reaction conditions, although the selectivity to 1,2-PDO was negligible and only unidentified products, probably polyglycerols and others degradation compounds, were mainly formed. On the other hand, the pure Cu system showed moderate glycerol conversion values (*ca.*12%), but low selectivity and yield to 1,2-PDO. Concerning the bimetallic CuZr catalysts, no significant differences in glycerol conversion values were found (around 10%). On the contrary yields to 1,2-PDO were largely affected by the catalyst composition. Thus, measured yield reach maximum values (*ca.*10.5%) for 2.5CuZr and 6CuZr, being the selectivity values for these catalysts higher than 90%.

It should be mentioned that here only has been represented the yield to 1,2-PDO, the main reaction product, however for different samples other reaction products as acetol and ethylene glycol (selectivity lower than 2%) were also detected. A detailed scheme with the different reaction products and co-products can be found in the open literature [1,2].

By the other hand it is clear that a fraction of reaction products cannot be identified and quantified by GC, at least for samples with worse catalytic performance. To shed some light about complete product distribution we have determined the H_2O concentration in the final reaction liquid by Karl Fisher titration. We found that this H_2O concentration after reaction was higher than expected considering the H_2O molecules released during glycerol dehydration reactions to form 1,2-PDO. The excess of H_2O may be due to glycerol condensation reactions to yield polyglycerols and/or to secondary dehydration reactions resulting in the formation of heavy products, undetectable by GC [9].

The activated CuZr catalysts were characterized aiming to explain the observed behavior in glycerol hydrogenolysis. Fig. 6 shows the XRD patterns recorded with the *x*CuZr samples treated in H_2/Ar at 573 K for 1 h and subsequently passivated at room temperature K in flowing 3 vol.% O_2/Ar for more than 1 h. The Cu-free and low Cu content solids (ZrO_2, 0.2CuZr, and 0.4CuZr) exhibit the broad diffraction peak ($2\theta = 20–40°$) attributed to low-crystalline ZrO_2 (1), the Cu-free sample also presents minor concentrations of crystalline cubic ZrO_2 (2). As the Cu loading increases, diffraction peaks attributed to metallic Cu (3), JCPDS 085–1326) become more apparent. Cu crystal sizes for 0.4CuZr, 1CuZr, 2.5CuZr, 6CuZr, and Cu samples calculated by applying the Scherrer equation to the diffraction line at $2\theta = 43.3°$ are reported in Table 1. ZrO_2 favors

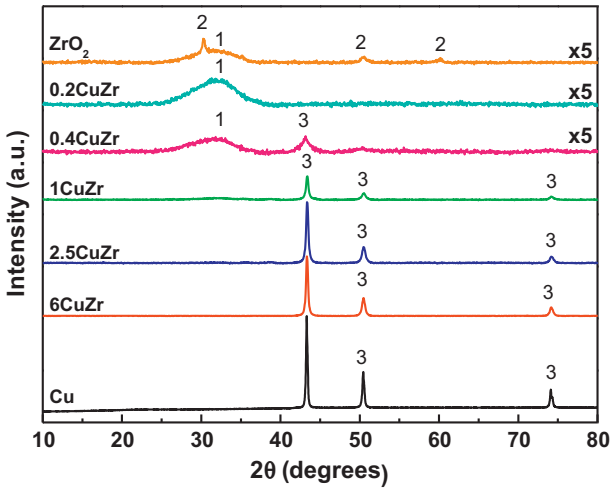

Fig. 6. XRD patterns of the *x*CuZr solids treated in 5 vol.% H_2/Ar at 573 K for 1 h. Phases identification: (1) low-crystalline ZrO_2; (2) cubic ZrO_2; (3) metallic Cu.

Please cite this article in press as: D. Durán-Martín, et al., Stability and regeneration of Cu–ZrO_2 catalysts used in glycerol hydrogenolysis to 1,2-propanediol, Catal. Today (2013), http://dx.doi.org/10.1016/j.cattod.2012.11.013

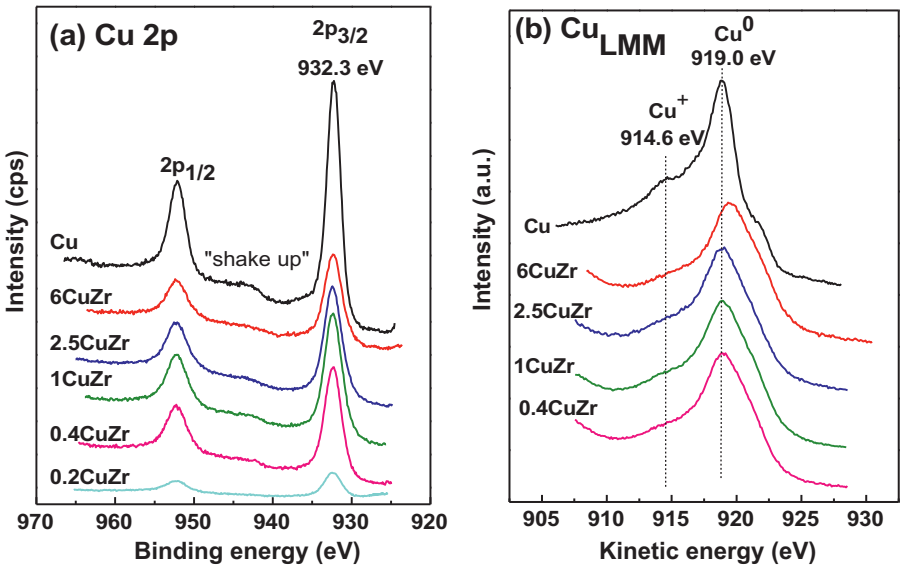

Fig. 7. Cu 2p XPS (a) and Cu_{LMM} Auger (b) spectra obtained for the *x*CuZr solids treated in 5 vol.% H_2/Ar at 573 K for 1 h.

the formation of smaller Cu crystallites [12]. This is evidenced by comparing the size of CuO or Cu particles for the unreduced and reduced samples (Table 1). In the first case, CuO crystallites for the bimetallic *x*CuZr samples are of *ca.* 10 nm, which yielded 20–30 nm Cu particles after the H_2/Ar treatment. This agglomeration effect is more significant in the monometallic Cu sample, in which CuO particles (*ca.* 12 nm) sinter during the reduction process to gives metallic Cu particles of *ca.* 50 nm. Moreover the size of Cu particles decreases in those solids with lower Cu/Zr atomic ratios.

X-ray photoelectron and Auger electron spectra of the *x*CuZr samples treated in H_2/Ar (573 K, 1 h) are depicted in Fig. 7. In all samples, the binding energy of the Cu $2p_{3/2}$ peak appears at 932.3 eV (Fig. 7a), which can correspond to both Cu^0 and Cu^+ species. The presence of Cu^{2+} is discarded, as evidenced by the absence of a satellite peak at *ca.* 942.9 eV [20,21]. Auger Cu_{LMM} spectra (Fig. 7b) allow to determine the identity of the copper species. The observed broadening of the Auger peaks with the Zr content is the result of the increasing overlapping with the Zr $3p_{1/2}$ peak [22]; this effect is especially significant for the 0.2CuZr sample and consequently, the Auger Cu_{LMM} spectrum does not provide much information about the chemical identity of Cu species in this case. For the rest of bimetallic samples, a broad peak centered at 919.0 eV suggests the presence of Cu^0 [23,24]. The monometallic Cu solid exhibits an additional small peak at 914.6 eV, indicative of a minor concentration of Cu^+ species, not detectable in the bimetallic samples. In summary, XPS and Auger spectra of the CuZr samples demonstrate the predominant presence of metallic copper (Cu^0) on the solids surface, although a much lower amount of Cu^+ is also detected for the pure Cu sample.

A detailed summary of the analysis of the most relevant XPS features (Cu $2p_{3/2}$, O 1s, Zr $3d_{5/2}$, and Cu/Zr atomic ratio) is presented in Table 2. The binding energy of the Zr $3d_{5/2}$ region (182.2 eV) is attributed to Zr^{4+} species as ZrO_2 [25]. Two components, centered at 530.0 and 532.0 eV, are distinguished in the O 1s core level, assigned respectively to network and hydroxyls/carbonates oxygen atoms [26]. These latter species may correspond either to surface OH groups or to the hydroxycarbonates species that remain on the catalyst surface after the thermal treatment step required to activate the catalysts. Table 2 also collects the Cu/Zr atomic ratios obtained from XPS data. This atomic ratio is increased with the copper content, but for the binary catalyst with higher content 2.5CuZr and 6CuZr was 0.7 and 1.1 respectively, being significantly lower than the theoretical bulk composition, which is consistent with the agglomeration of the copper particles observed by XRD.

Despite the characterization effort, for CuZr catalytic system there is not well defined trend between glycerol conversion and the composition of the catalyst. As regards the selectivity to 1,2-PDO, significantly increases was observed for catalysts with Cu/Zr ≥ 1, reaching values higher than 90%. The particle size of metallic copper (between 20 and 30 nm) along with the surface atomic ratio Cu/Zr (about 1) are the two peculiarities of these bimetallic catalysts. These results suggest that increasing of the Cu/Zr ratio increases the amount of surface exposed copper and therefore an increase in selectivity. When there is sufficient amount of copper present practically unchanged selectivity being independent of the composition.

3.3. Deactivation and regeneration of CuZr catalysts for glycerol hydrogenolysis

To study the stability of these catalysts and their possible regeneration, 6CuZr sample, one of which showed better catalytic performance, has been chosen to reusing for several cycles of reaction. Fig. 8 reports the catalytic behavior of 6CuZr used in glycerol

Table 2
Binding energy (eV) and Cu/Zr atomic ratios measured with the CuZr samples treated in H_2/Ar (573 K, 1 h) by XPS data.

Sample	Binding energy (eV)			Cu/Zr atomic ratio
	Cu $2p_{3/2}$	O 1s [a]	Zr $3d_{5/2}$	
ZrO_2	–	530.0 (66) 531.6 (34)	182.2	–
0.2CuZr	932.4	530.0 (71) 531.4 (29)	182.3	0.1
0.4CuZr	932.3	530.0 (69) 532.3 (31)	182.4	0.6
1CuZr	932.3	530.0 (67) 531.7 (33)	182.3	0.8
2.5CuZr	932.3	530.1 (75) 532.1 (25)	182.3	0.7
6CuZr	932.3	530.0 (64) 531.7 (36)	182.3	1.1
Cu	932.4	533.1	–	–

[a] Values in brackets indicate the percentage of each component.

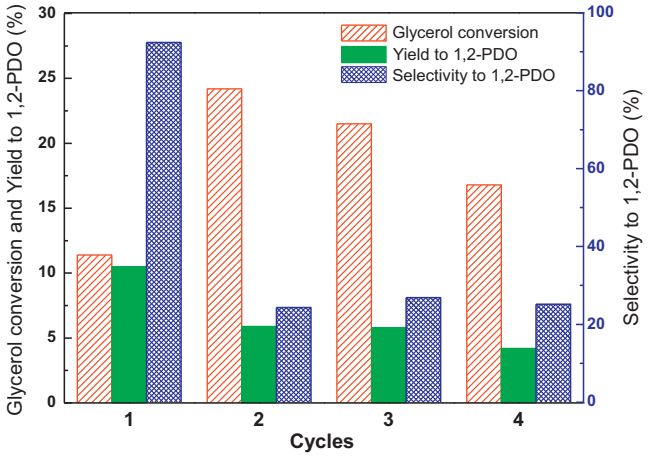

Fig. 8. Catalytic performance shown by the *x*CuZr solids used in consecutive glycerol hydrogenolysis cycles (10 g glycerol, 15 g H_2O, 4.0 MPa H_2, 0.6 g catalyst, 473 K, 8 h).

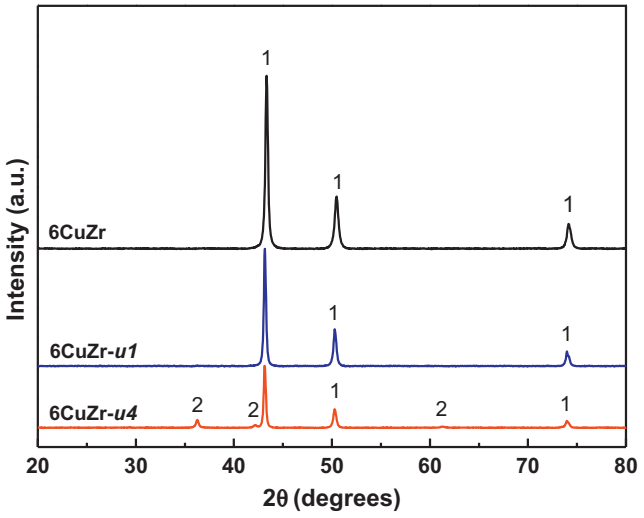

Fig. 9. XRD patterns of the fresh activated 6CuZr catalyst and after use in glycerol hydrogenolysis (10 g glycerol, 15 g H_2O, 4.0 MPa H_2, 0.6 g catalyst, 473 K, 8 h) for 1 and 4 catalytic cycles. Phases identification: (1) metallic Cu; (2) Cu_2O.

hydrogenolysis for up to four cycles. Experimentally, the catalyst was allowed to settle down after each reaction test, separated from the reaction medium and used subsequently with a fresh aqueous solution of glycerol without being submitted to any washing or reactivation step. Although conversion increases, the selectivity and yield to 1,2-PDO decreased drastically for the second run (from 92.4 to 24.3%, and from 10.5 to 5.9%, respectively). For further cycles, the rate of deactivation is not so intense and the catalytic properties in successive cycles worsen in a smoother manner.

Next, the solids recovered after the first and fourth catalytic cycles (named with the suffixes *–u1* and *–u4*, respectively) were submitted to chemical analysis, XRD and XPS characterization techniques to identify the deactivation phenomena that occur, and eventually, find an appropriate experimental procedure to successfully reactivate the catalysts.

First, the catalysts were analyzed by TXRF, and it was found that the chemical composition of the solid used for 4 cycles (6CuZr-*u4*) did not change (83.6% Cu, 16.4% Zr, percentages are relative to metal atoms) compared to the fresh catalyst (83.3% Cu, 16.7% Zr). Furthermore, ICP-MS analysis of the reaction liquids gave Cu and Zr contents lower than 0.1 ppm, which allows us to rule out leaching as the relevant deactivation cause. Furthermore, we have found in a parallel investigation with other Cu based catalyst prepared by coprecipitation as well that Cu leaching occurs because of the formation of complexes with lactic acid molecules originated in glycerol hydrogenolysis [10]. In the present work, we have not detected any significant variation of pH after each catalytic cycle with 6CuZr, suggesting that Cu leaching by lactic acid is not relevant. It is necessary to emphasize the positive effect of the use of zirconium oxide in these systems in relation to the possible deactivation by leaching.

Fig. 9 depicts the XRD patterns obtained with the fresh and used 6CuZr catalysts, showing that copper particles remain in the metallic state (Cu^0) after the first and fourth cycles, although minor formation of Cu_2O (JCPDS 078–2076, 25.8 nm cluster size, $2\theta = 36.4^\circ$) is also detected in the latter case. On the other hand, Cu cluster size increases somewhat from 20.5 nm (6CuZr; $2\theta = 50.4^\circ$, in this case the main reflection $2\theta = 43.3^\circ$ has not been considered to apply the Scherrer equation because it may be affected by a reflection from Cu_2O at $2\theta = 42.3^\circ$) to 27.5 and 28.5 nm (6CuZr-*u1* and 6CuZr-*u4*, respectively). The slight sintering of Cu particles detected by XRD, although it may have certain impact on the deactivation, is not as significant as to explain the observed remarkable decreased in the measured selectivity to 1,2-PDO. In fact, the Cu/Zr atomic ratio measured by XPS remain mostly constant, 1.1 and 1.2 for the fresh (6CuZr) and used (6CuZr-*u1*, 6CuZr-*u4*) catalysts, suggesting that copper species do not agglomerate significantly under the reaction conditions.

X-ray photoelectron and Auger electron spectra of the fresh and used 6CuZr samples are depicted in Fig. 10. The analysis of the Cu 2p region (Fig. 10a) reveals the exclusive presence of Cu^0 and/or Cu^+ species (Cu $2p_{3/2}$ = 932.3 eV) in the solids used for 1 and 4 catalytic cycles (BE of Cu 2p corel level is the same for Cu^0 and Cu^+ species). These data also reveal that Cu^{2+} species are not formed, evidenced by the absence of the characteristic satellite "shake-up" features [20,21]. Therefore, we conclude that catalysts deactivation is not caused by metallic Cu^0 oxidation to CuO. The Auger Cu_{LMM} spectra shown in Fig. 10b confirm that, consistent with XRD, metallic Cu^0 species exist predominantly in the 6CuZr and 6CuZr-*u1* catalysts, while Cu^+ is additionally detected for the 6CuZr-*u4* sample (also in agreement with XRD). Nonetheless, the formation Cu_2O does not seem to exhibit a significant impact on catalysts deactivation because deactivation occurs predominantly during the first catalytic run (Fig. 8), while Cu_2O is only detected after the fourth reaction cycle (Figs. 9 and 10).

The C 1s region of the X-ray photoelectron spectrum (Fig. 11) recorded with the fresh 6CuZr sample displays a single peak at 284.6 eV due to adventitious hydrocarbon species adsorbed on the surface. Interestingly, 6CuZr-*u1* and 6CuZr-*u4* solids present an additional peak at 289.5 eV, which intensity clearly increases with the number of catalytic cycles, and that is attributed to carbonaceous residues deposited during the catalytic reaction. Therefore, the blocking or the poisoning of catalytically active sites by reaction intermediates and/or products seems to be the most relevant deactivation cause. In summary the formation of organic deposits is mostly responsible for the observed decay of the catalytic activity.

Accordingly and concerning to regeneration process, we have investigated different catalyst reactivation protocols to remove the organic molecules deposited over the catalyst surface to thus recover the initial catalyst activity displayed by the 6CuZr solid. It was submitted to the following regeneration processes: calcination in synthetic air at 673 K for 1 h under a rapid heating ramp (10 K/min) (process a) and under a slow heating ramp (1 K/min) (process b) and subsequent treatment in H_2/Ar flow (5 vol. %, 5 K min^{-1}, 573 K, 1 h) for both. The objective of the treatment step in O_2 is to burn the organic deposits, while the H_2 process aims to re-form the metallic Cu^0 particles. During all these protocols, the gases evolved from the sample were analyzed with mass

Please cite this article in press as: D. Durán-Martín, et al., Stability and regeneration of Cu–ZrO_2 catalysts used in glycerol hydrogenolysis to 1,2-propanediol, Catal. Today (2013), http://dx.doi.org/10.1016/j.cattod.2012.11.013

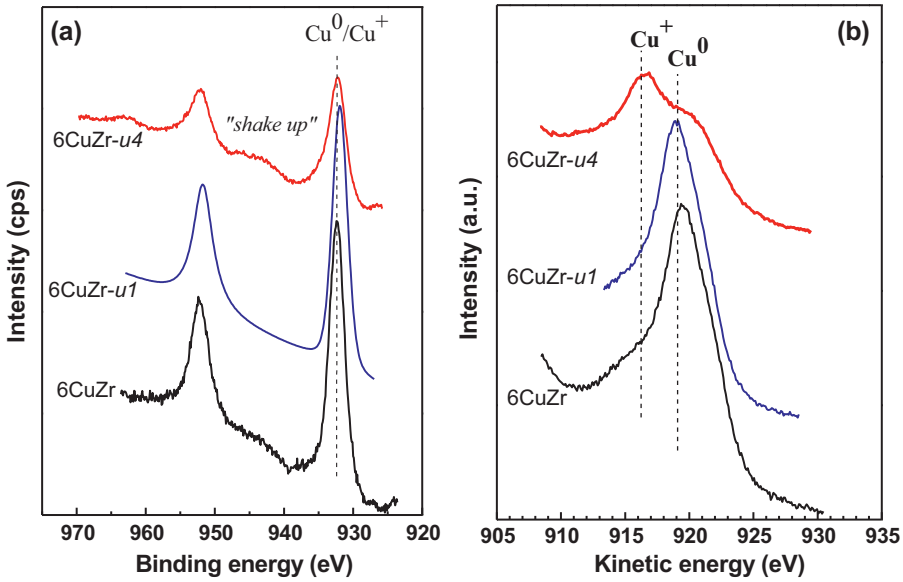

Fig. 10. Cu 2p XPS (a) and Cu_{LMM} Auger (b) spectra obtained for the fresh activated 6CuZr catalyst and after use in glycerol hydrogenolysis (10 g glycerol, 15 g H_2O, 4.0 MPa H_2, 0.6 g catalyst, 473 K, 8 h) for 1 and 4 catalytic cycles.

spectrometer (not shown here). When the calcination step in O_2/Ar is performed at relatively high heating rates (10 K min^{-1}, procedure a), an exothermic combustion of organic deposits (formation of H_2O and CO_2) present on the catalyst surface was observed, and may probably cause the irreversible sintering of copper crystallites. In contrast, a linear and controlled temperature increase (from 298 to 673 K) and the absence of CO_2 formation is noticed when very low heating rates (1 K min^{-1}) are used, so under these conditions the organics deposits were not combusted. This means that surface hydrocarbons are being oxidized but still remains at the surface either poisoning or fouling the surface. The formation of partially oxidized hydrocarbons (with alcohol, carbonyl and/or acid functions) seems very likely, all the latter species with capacity to chelating metallic species and therefore resulting in a poisoning of the active sites. A third regeneration process consisted in the thermal treatment of the spent CuZr catalysts with a H_2/Ar 5 vol. % H_2/Ar flow (5 K min^{-1}, 573 K, 1 h) (process c), without a previous O_2/Ar calcination step. The solids regenerated were labeled with the suffixes *-ra, -rb* and *–rc*, to make reference to the processes a, b and c respectively.

Fig. 12 displays the catalytic behavior of the 6CuZr spent catalyst, used during 4 cycles, after undergoing to the different regeneration protocols. Catalytic data for the first reaction cycle (fresh catalyst) is also depicted for comparison. First of all, we observe that the O_2/Ar treatment at 673 K for 1 h (heating rate of either 1 or 10 K min^{-1}) does not lead to the 1,2-PDO yield measured during the first catalytic cycle (*ca.* 5% *versus* 10.5%). However, we have found that the reactivation of the spent CuZr catalyst (6CuZr-*u4*) in H_2/Ar (573 K, 1 h) allows us to successfully recuperate the initial measured yields (9% *versus* 10.5%). It seems very likely that this relatively simple treatment protocol (H_2/Ar flow, 5 K min^{-1} up to 573 K, 1 h) efficiently gasifies and removes by hydrogenation the organic

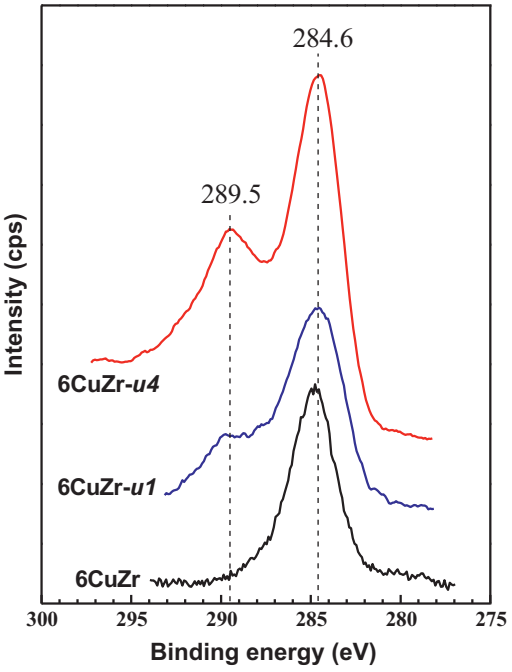

Fig. 11. C 1s region of the X-ray photoelectron spectra obtained for the fresh activated 6CuZr catalyst and after use in glycerol hydrogenolysis (10 g glycerol, 15 g H_2O, 4.0 MPa H_2, 0.6 g catalyst, 473 K, 8 h) for 1 and 4 catalytic cycles.

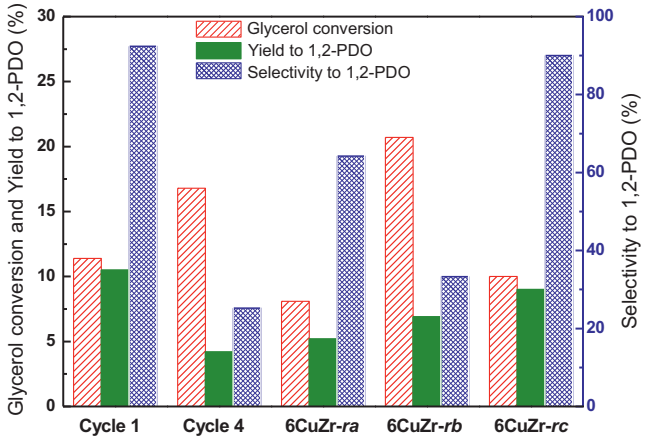

Fig. 12. Catalytic performance shown by the 6CuZr spent catalyst (used for 4 cycles) and after its regeneration by different protocols (a, b and c) in glycerol hydrogenolysis (10 g glycerol, 15 g H_2O, 4.0 MPa H_2, 0.6 g catalyst, 473 K, 8 h). Data for the fresh catalyst is also depicted for comparison.

Please cite this article in press as: D. Durán-Martín, et al., Stability and regeneration of Cu–ZrO_2 catalysts used in glycerol hydrogenolysis to 1,2-propanediol, Catal. Today (2013), http://dx.doi.org/10.1016/j.cattod.2012.11.013

molecules deposited on the catalyst surface without affecting significantly the identity and nature of the active sites. Since metallic Cu species are mostly responsible for the selectivity to 1,2-PDO [9] a reasonable explanation of the good performance for the regeneration process c should be associated with the selective removal of carbonaceous deposits on the metallic Cu species. In any case a more detailed work would be needed to clarify it.

4. Conclusions

The catalysts with higher copper content, 2.5CuZr and 6CuZr, show the better catalytic behavior in the hydrogenolysis of glycerol, with a high selectivity to 1,2-PDO, more than 90%, at a conversion around the 10% and under the reaction conditions employed in this work.

The stability of the CuZr catalytic system in the reaction medium has been studied for one of the most active catalysts of the series, 6CuZr. This catalyst is quite stable during its use in the hydrogenolysis in terms of absence of leaching of the components of the catalyst in the reaction medium. A slight oxidation and sintering of copper after four runs of the reutilization reaction have been observed. Nevertheless, the 1,2-PDO yield decrease after the first run of reaction is attributed to the progressive formation of organic deposits on the surface of the catalyst. The carbonaceous deposits seem to be located on the metallic Cu species since the deactivation is due mainly to 1,2-PDO selectivity decrease.

This cause of deactivation is reversible and it has demonstrated that the catalyst can be regenerated by applying a reduction thermal under H_2 treatment, thus a substantial recovering of the yield to 1,2-PDO shown by the fresh catalyst was achieved.

Acknowledgements

Financial support from Spanish Ministry of Science and Innovation (ENE2009-12743-C04-01 and RYC-2010-06067) and Autonomous Government of Madrid (S2009/ENE-1660, CARDENER-CM partly funded by FSE funds) is gratefully acknowledged. D.D.M. thanks the Spanish Ministry of Education for her FPU fellowship.

References

[1] Y. Nakagawa, K. Tomishige, Catalytic Science and Technology 1 (2011) 179–190.
[2] J. ten Dam, U. Hanefeld, ChemSusChem 4 (2011) 1017–1034.
[3] J. Chaminand, L. Djakovitch, P. Gallezot, P. Marion, C. Pinel, C. Rosier, Green Chemistry 6 (2004) 359–361.
[4] S. Wang, Catalysis Letters 117 (2007) 62–67.
[5] M. Balaraju, V. Rekha, P.S. Sai Prasad, N. Lingaiah, Catalysis Letters 126 (2008) 119–124.
[6] Z. Huang, F. Cui, H. Kang, J. Chen, X. Zhang, C. Xia, Chemistry of Materials 20 (2008) 5090–5099.
[7] S. Sato, M. Akiyama, R. Takahashi, T. Hara, K. Inui, M. Yokota, Applied Catalysis A: General 347 (2008) 186–191.
[8] I. Gandarias, P.L. Arias, J. Requies, M. El Doukkali, M.B. Güemez, Journal of Catalysis 282 (2011) 237–247.
[9] F. Vila, M. López Granados, M. Ojeda, J.L.G. Fierro, R. Mariscal, Catalysis Today 187 (2012) 122–128.
[10] D. Durán-Martín Glycerol hydrogenolysis to 1,2-propanediol with binary copper catalysts, Ph.D. Thesis, Autonomous University of Madrid, Spain, 2011.
[11] R.A. Koeppel, A. Baiker, Applied Catalysis A: General 84 (1992) 77–102.
[12] Y. Sun, P.A. Sermon, Catalysis Letters 29 (1994) 361–369.
[13] M. Shimokawabe, H. Asakawa, N. Takezawa, Applied Catalysis 59 (1990) 45–58.
[14] D.L. Hoang, H. Lieske, Catalysis Letters 27 (1994) 33–42.
[15] C. Dall'Agnol, A. Gervasini, F. Morazzoni, F. Pinna, G. Strukul, L. Zanderighi, Journal of Catalysis 96 (1985) 106–114.
[16] J.P. Breen, J.R.H. Ross, Catalysis Today 51 (1999) 521–533.
[17] C.Z. Yao, L.C. Wang, Y.M. Liu, G.S. Wu, Y. Cao, W.L. Dai, H.Y. He, K.N. Fan, Applied Catalysis A: General 297 (2006) 151–158.
[18] A. Szizybalski, F. Girgsdies, A. Rabis, Y. Wang, M. Niederberger, T. Ressler, Journal of Catalysis 233 (2005) 297–307.
[19] M. Turco, G. Bagnasco, C. Cammarano, P. Senese, U. Costantino, M. Sisani, Applied Catalysis B: Eironmental 77 (2007) 46–57.
[20] D.C. Frost, A. Ishitani, C.A. McDowell, Molecular Physics: An International Journal at the Interface Between Chemistry and Physics 24 (1972) 861–877.
[21] T.H. Fleisch, G.J. Mains, Applied Surface Science 10 (1982) 51–62.
[22] H.W. Chen, J.M. White, J.G. Ekerdt, Journal of Catalysis 99 (1986) 293–303.
[23] N.S. McIntyre, M.G. Cook, Analytical Chemistry 47 (1975) 2208–2213.
[24] C.D. Wagner, Analytical Chemistry 47 (1975) 1201–1203.
[25] Z. Liu, M.D. Amiridis, Y. Chen, Journal of Physical Chemistry B 109 (2005) 1251–1255.
[26] C.D. Wagner, A.V. Naumkin, A. Kraut-Vass, J.W. Allison, C.J. Powell, J.R. Rumble Jr., NIST Standard Reference Database 20, Version 3.4 (Web Version). http://srdata.nist.gov/xps/

Please cite this article in press as: D. Durán-Martín, et al., Stability and regeneration of Cu–ZrO_2 catalysts used in glycerol hydrogenolysis to 1,2-propanediol, Catal. Today (2013), http://dx.doi.org/10.1016/j.cattod.2012.11.013